Electronic Supplementary Information (ESI)

Expanding the aqueous-based redox-facilitated self-polymerization chemistry of catecholamines to 5,6-dihydroxy-1H-benzimidazole and its 2-substituted derivatives

Ka Wai Fan,[a] Matthew B. Peterson,[b] Peter Ellersdorfer,[a] Anthony M. Granville*[a]

[a] Centre for Advanced Macromolecular Design, School of Chemical Engineering, The University of New South Wales, Kensington, NSW 2052, Australia.

Email: a.granville@unsw.edu.au

[b] School of Chemistry, The University of New South Wales, Kensington, NSW 2052, Australia

SI 1. Characterization

1.1. ^{1}H, ^{13}C, ^{19}F and 2D Nuclear Magnetic Resonance (NMR) Spectroscopy

All solution-based NMR analyses were performed on a Bruker Avance III 300 MHz spectrometer equipped with a SampleXpress automatic sample changer and BBFO z-gradient probe. The samples were dissolved in deuterated solvents [either chloroform-d_1 ($CDCl_3$, D-99.8%) or dimethyl sulfoxide-d_6 (DMSO-d_6, D-99.9%) depending on the solubility] supplied by Cambridge Isotope Laboratories, Inc. ^{1}H NMR spectra were acquired at 300 MHz with a minimum of 8 scans, ^{13}C NMR spectra were acquired at 75 MHz with a minimum of 256 scans, and ^{19}F NMR spectra were acquired at 282 MHz with a minimum of 16 scans. For 2D NMR, heteronuclear single-quantum correlation (HSQC) and heteronuclear multiple-bond correlation (HMBC) were performed. The results were plotted against each other with ^{1}H spectrum as x-axis and ^{13}C spectrum as y-axis to elucidate the structure.

1.2. ^{13}C CP-MAS Solid State NMR (SSNMR) Spectroscopy

All SSNMR analyses were performed on a Bruker Avance III 300 Solid State spectrometer equipped with a 4 mm 1H/X broadband CP-MAS (cross polarization-magic angle spinning) probe. The samples were densely packed into 4 mm o.d. rotors, which were spun at 8 kHz for analyses. The ^{13}C spectra were acquired with 3 μs recycle delay and 13 ms acquisition time. SPINAL64 was chosen as the ^{1}H decoupling mode. 3072 scans were performed for the polymer and copolymer samples while 1024 scans were performed for 5,6-dihydroxy-*1H*-benzimidazole. The acquired spectra were referenced to the carbonyl peak at 176 ppm on the ^{13}C spectrum of glycine.

1.3. Cyclic Voltammetry (CV)

The voltammograms were acquired with an eDAQ Integrated Potentiostat System (ER466) equipped with an Ag/AgCl reference electrode, and platinum counter and working electrodes. The unit was controlled with EChem Software (eDAQ Pty Ltd). Concentration of the sample and buffer solution was the same as that of the polymerization. The sample was scanned at 400 mV s^{-1} and 26 scans were performed until changes in the cycles were no longer observed.

1.4. Dynamic Light Scattering (DLS)

Particle size distribution and zeta potential were measured by a Malvern Zetasizer Nano ZS equipped witha 4mW He-Ne laser (λ = 632.8 nm). The instrument was calibrated with titanium oxide standard (RI = 2.40, absorption = 0.01). At least three measurements were performed on each sample, and each measurement consisted of 12 to14 scans. The sample was dispersed at low concentration in deionized water (RI = 1.33, absorption = 0.01) by sonication prior to analysis. All measurements used poly(dopamine) [RI = 1.59,[1] absorption = 0.01, (same values for the silica particle templates)] as the reference material since the RI of poly(5,6-didhydroxy-*1H*-benzimidazole) and the copolymer were unknown. Similar setting

was applied for zeta potential measurements with Smoluchowski's theory chosen for the modeling. The number of scan in each measurement was set to automation.

1.5. Thermogravimetric Analysis (TGA)

Thermograms were obtained by TGA Q5000 (V3.15 Build 263) purchased from TA instruments. The sample was loaded onto a high-temperature platinum pan, which was then loaded into the furnace supplied with air (at 25.0 mL min^{-1}) and nitrogen (at 15.0 mL min^{-1}). The procedure was preprogrammed to ramp the temperature from 25 °C to 100 °C at 20 °C min^{-1}, and remain isothermal for 10 minutes to remove residual moisture in the sample. The temperature was then ramped from 100 °C to 900 °C at 10 °C min^{-1} to facilitate the thermal degradation of the sample. For the coated particles, the absolute weight loss was calculated by normalizing the maximum and minimum value to 100% and 0%, respectively

1.6. Transmission Electron Microscopy (TEM)

Images were acquired with a JEOL 1400 transmission electron microscope. The sample was dispersed at low concentration in deionized water with the aid of sonication. A drop of the dispersion was applied on the copper grid coated with formvar, and the dispersant was allowed to evaporate in air prior to perform imaging.

1.7. Electron Paramagnetic Resonance (EPR) spectroscopy

EPR was performed using a Bruker EMX-Plus X-Band ESR Spectrometer at 298 K using 100 kHz field modulation frequency and 100mT modulation amplitude.

1.8. Gel Permeation Chromatography (GPC)

GPC analyses were performed on a unit purchased from Shimadzu Scientific Instruments. *N,N*-dimethylacetamide was employed as the eluent [containing 0.3 g L^{-1} of lithium bromide and 0.5 g L^{-1} of 2,6-bis(1,1-dimethyl-ethyl)-4-methylphenol]. The sample was injected by a SIL-10AD VP auto-sampler at 50 μL, which eluted through the guard column (Phenomenex,

5 μm bead size) and the chromatography columns (Phenomenex, Phenogel – 10^5, 10^4 and 10^3 Å pore size) over 60 minutes using the LC-20AT pump. Temperature of the columns was regulated at 50 °C by a CTO-10A VP oven. A RID-10A refractive index (RI) detector was used to determine the molecular weight distribution of the sample. Regular calibration was performed on the unit with Polystyrene High EasiVials supplied by Agilent Technologies.

1.9. Contact Angle Measurement

Contact angle measurements were performed using a CAM200 Contact Angle and Surface Tension Meter, which was calibrated using a 4mm steel ball bearing as reference. Measurements were taken by applying a 10 μL drop of deionized water manually onto the level sample using a calibrated micropipette. At least three measurements were taken at different regions for each sample.

1.10. *Ultraviolet*-visible (UV-Vis) spectroscopy.

Absorption spectra were acquired by a Varian Cary 300 UV-Visible Spectrophotometer with a resolution of ≤ 0.24 nm. All samples were dispersed in deionized water and analyzed in a quartz cuvette unless specified.

1.11. Attenuated Total Reflectance Fourier Transform Infrared (ATR-FTIR) Spectroscopy

The spectra were acquired with a Bruker IFS 66/S single-beam spectrometer equipped with a mid-infrared lamp and diffuse reflectance sampling accessories. The resolution was set at 4 cm^{-1} and 32 scans were performed for each sample.

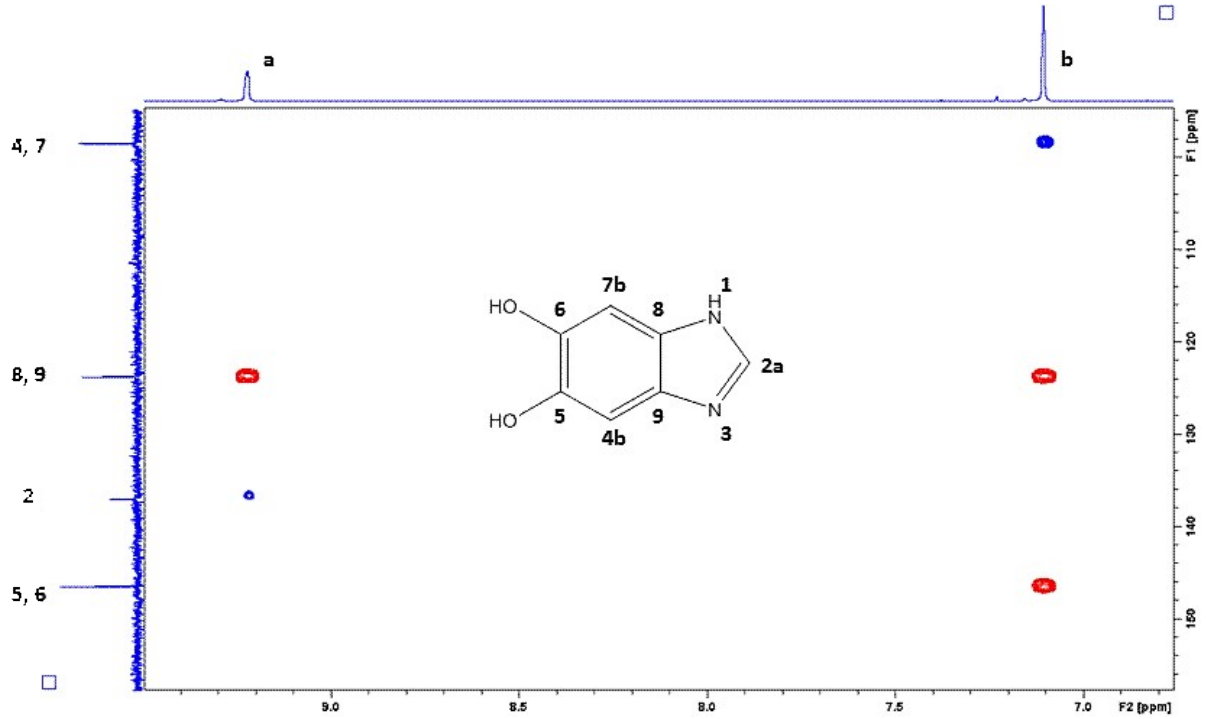

Fig. S1 Structure elucidation of DHBI by 2D NMR (HSQC – blue, HMBC – red).

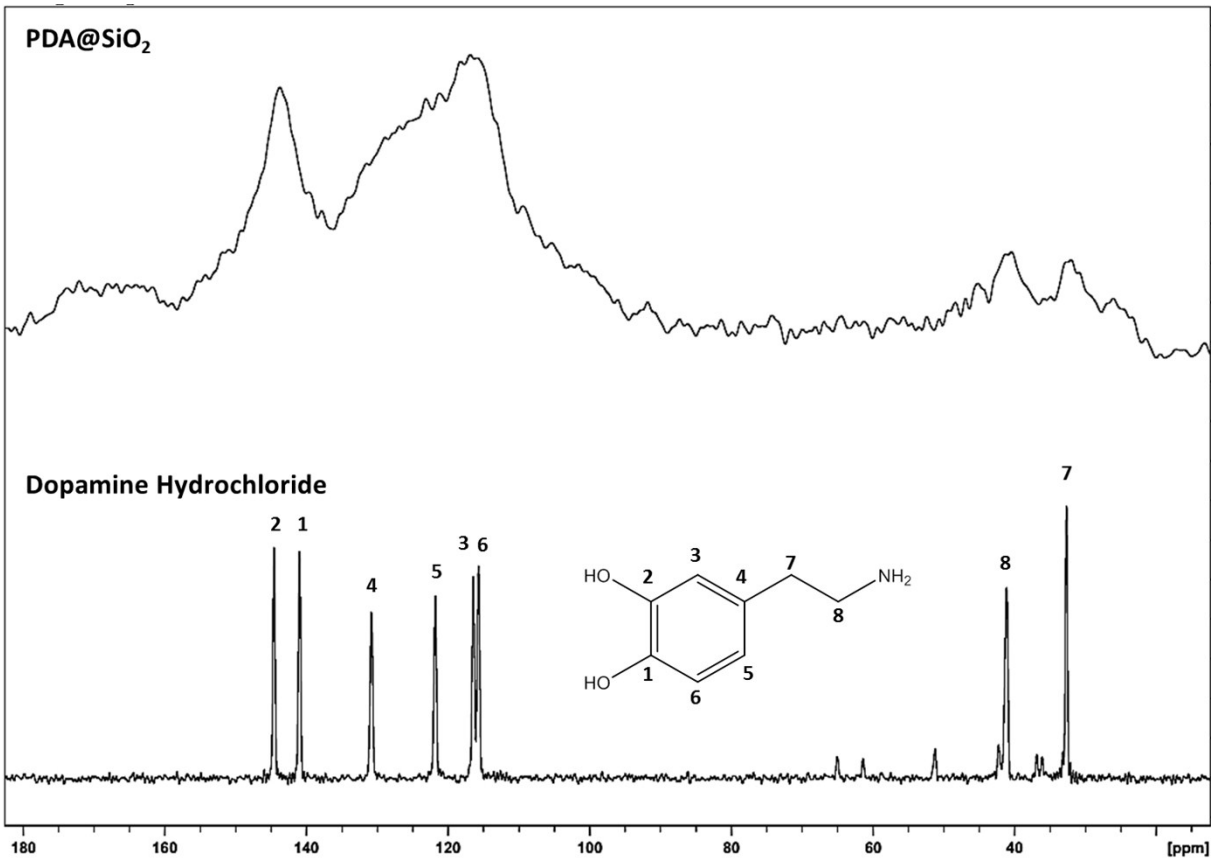

Fig. S2 Comparison of ^{13}C CP-MAS SSNMR spectra of dopamine hydrochloride and PDA@SiO_2.

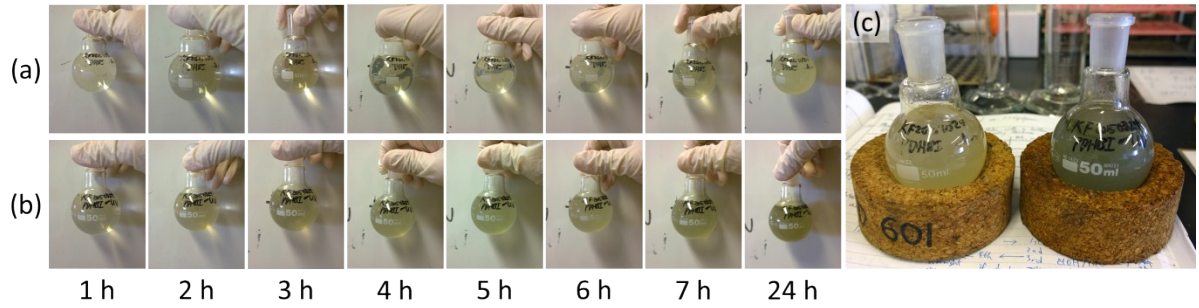

Fig. S3 Progressive changes in color and turbidity/translucency of the reaction mixtures observed from the DHBI self-polymerization under controlled (a) and the UV-stimulated (b) conditions, and a comparison of the appearance of the two samples (c, left = control, right = UV-stimulated) after 24 h.

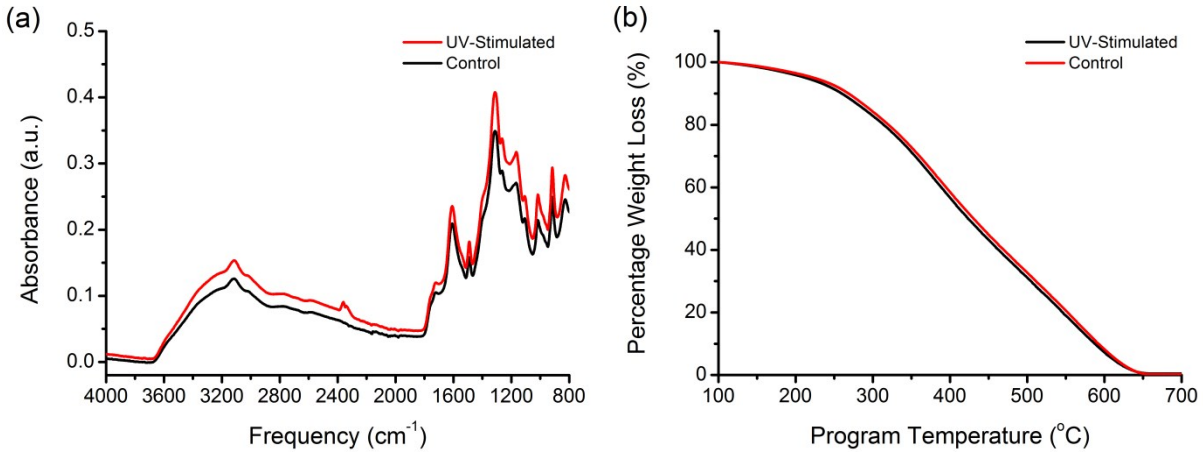

Fig. S4 ATR-FTIR (a) and TGA (b) results obtained for PDHBI prepared *via* UV-stimulation in comparison to the results obtained for the control sample.

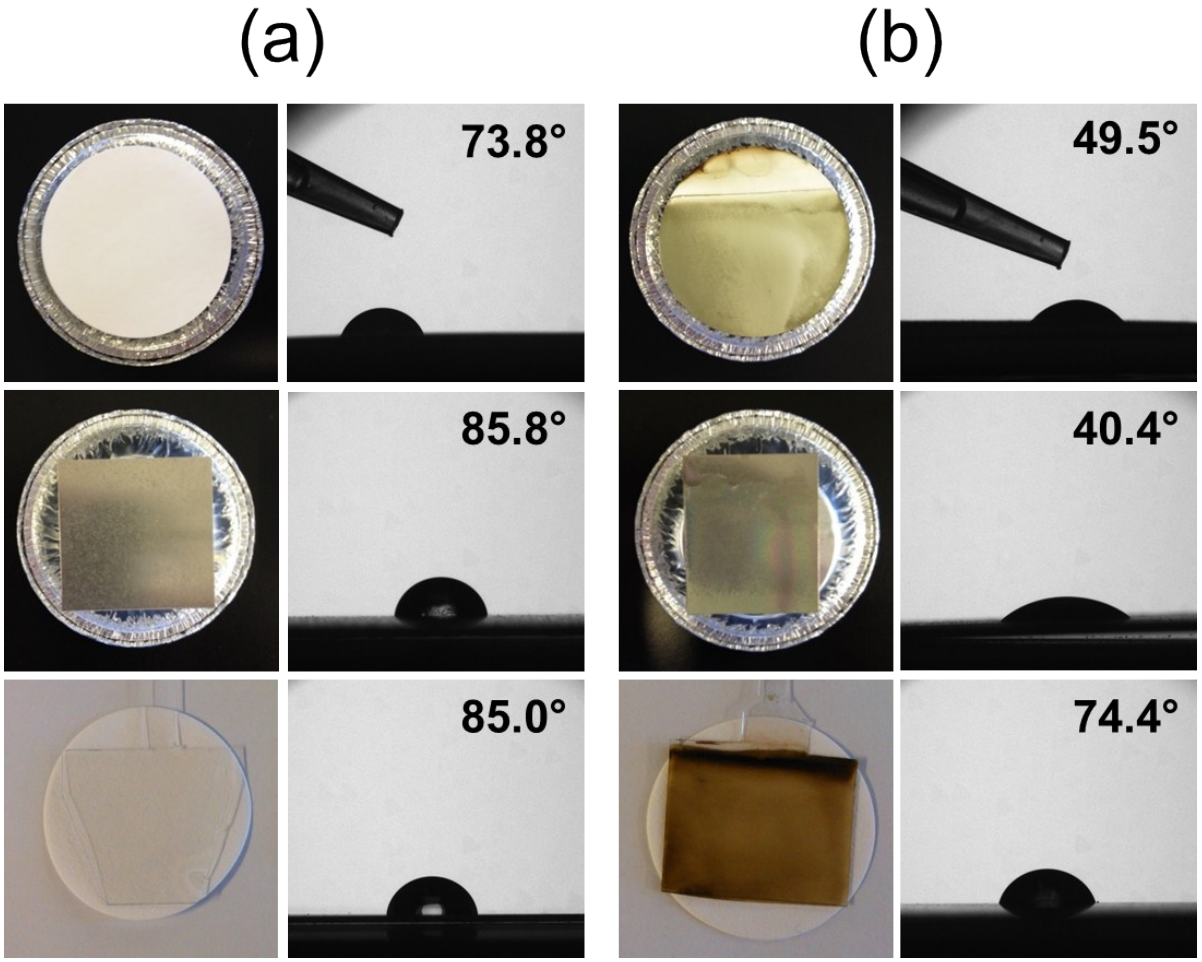

Fig. S5 Images and surface contact angle measurements of Millipore filter, stainless steel sheet, and PET film (top to bottom) before (a) and after (b) being coated with PDHBI.

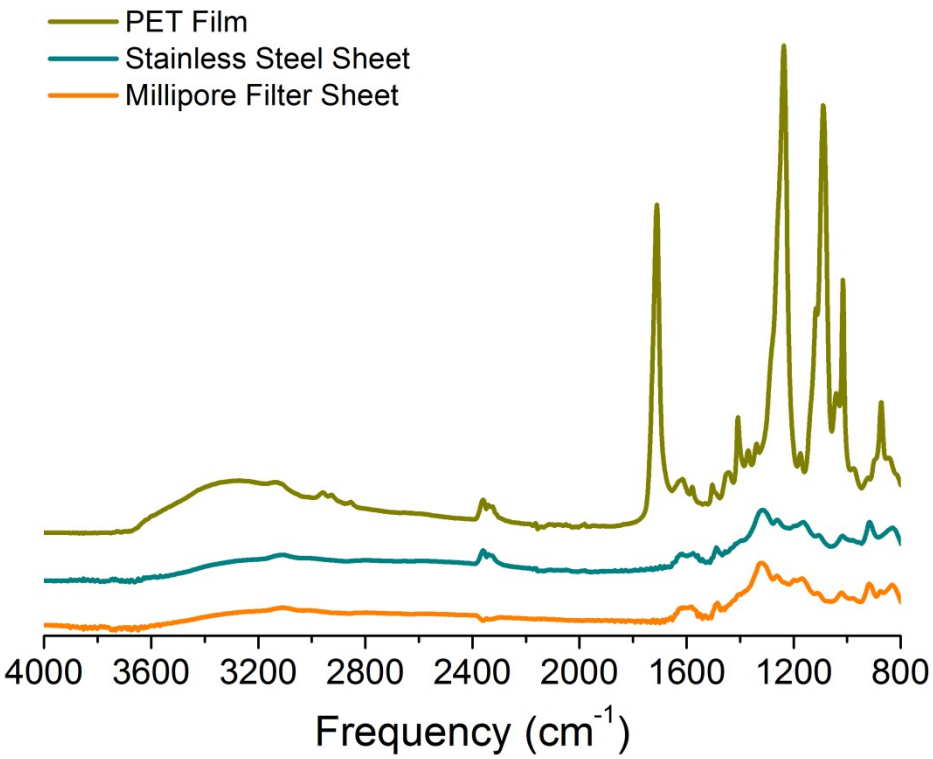

Fig. S6 ATR-FTIR spectra of PET film, stainless steel sheet and Millipore filter sheet coated with PDHBI.

Table S1 Contact angles measured from unmodified and PDHBI-coated materials

	Contact Angle, °		
Sample	**Millipore Filter Paper**	**Stainless Steel Sheet**	**PET Sheet**
Unmodified	73.8 ± 0.9	85.8 ± 0.7	85.0 ± 1.2
PDHBI-coated	49.5 ± 1.9	40.4 ± 0.6	73.1 ± 3.8 (1 coating) 74.4 ± 4.3 (3 coatings)

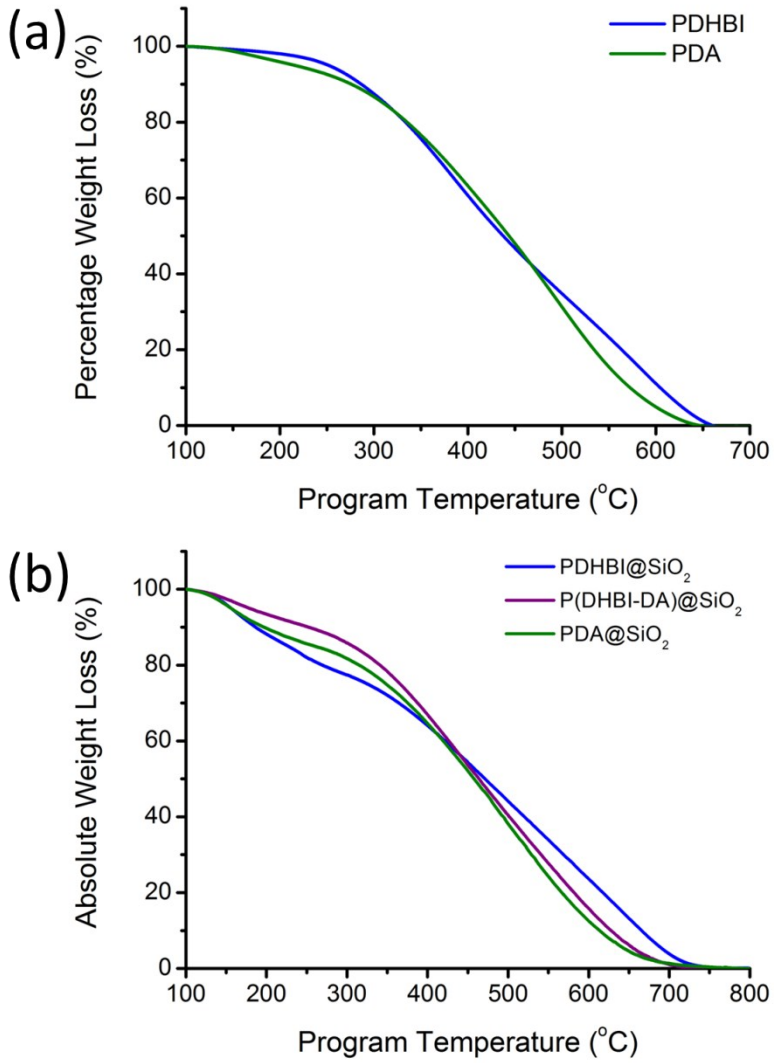

Fig. S7 Thermal degradation of homopolymers (a) and polymer-coated silica particles (b) acquired from TGA. Note that the results of the coated particles have been normalized to show absolute weight loss.

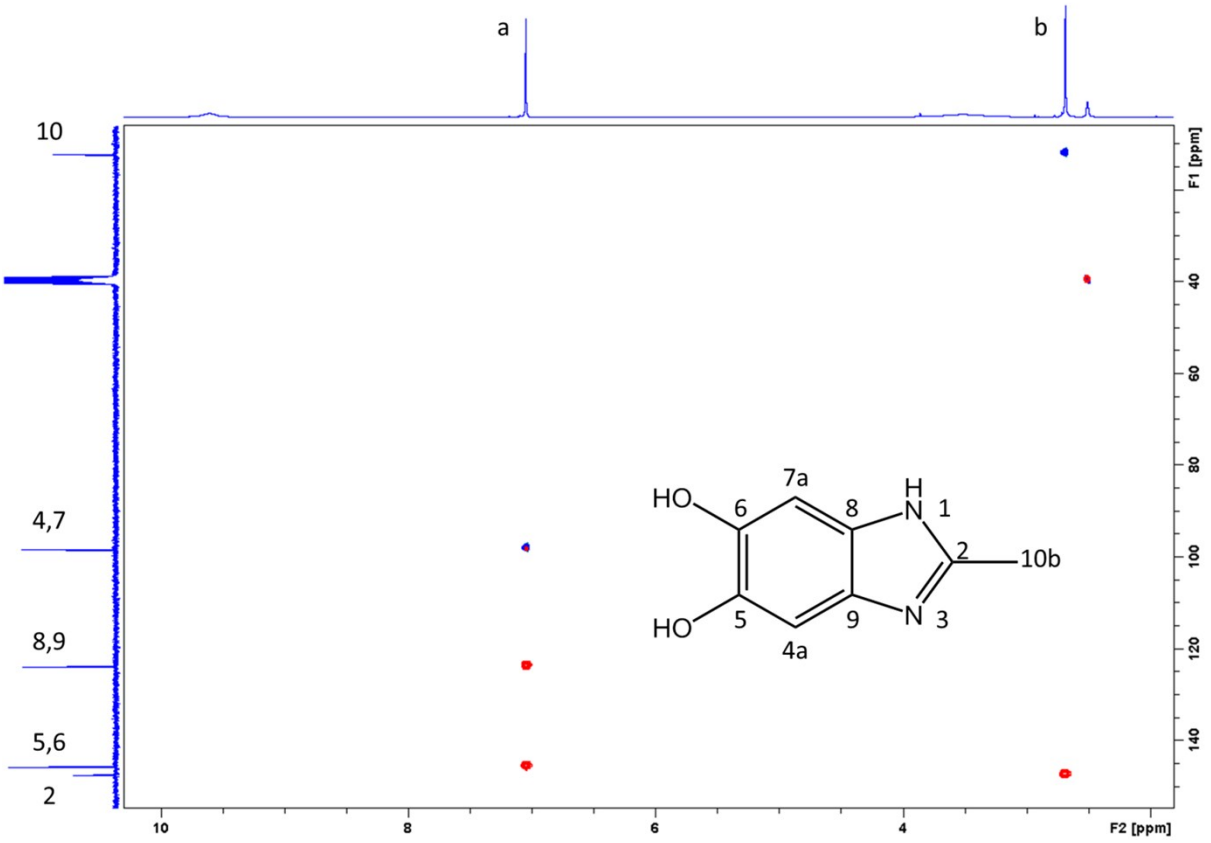

Fig. S8 Structure elucidation of 2-Me-DHBI by 2D NMR (HSQC – blue, HMBC – red).

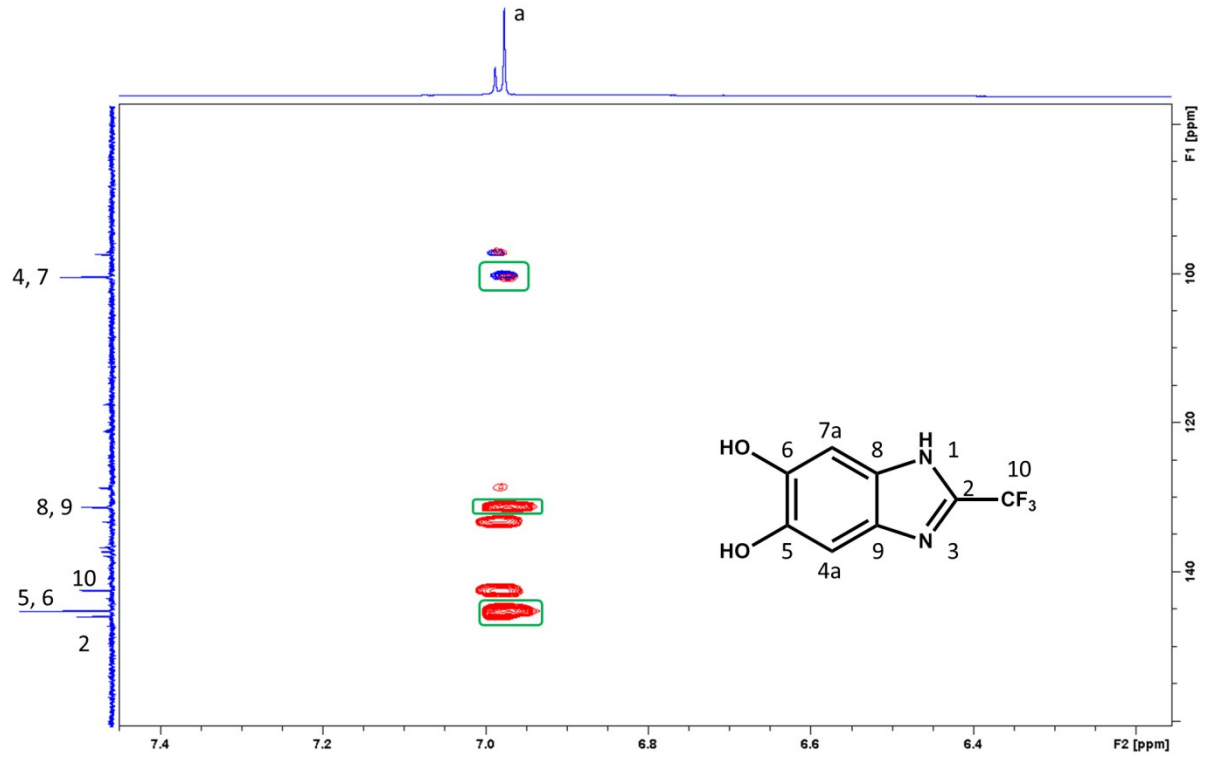

Fig. S9 Structure elucidation of 2-CF_3-DHBI by 2D NMR (HSQC – blue, HMBC – red). The corresponding correlations have been distinguished from the signals of the impurity with green rectangular outlines.

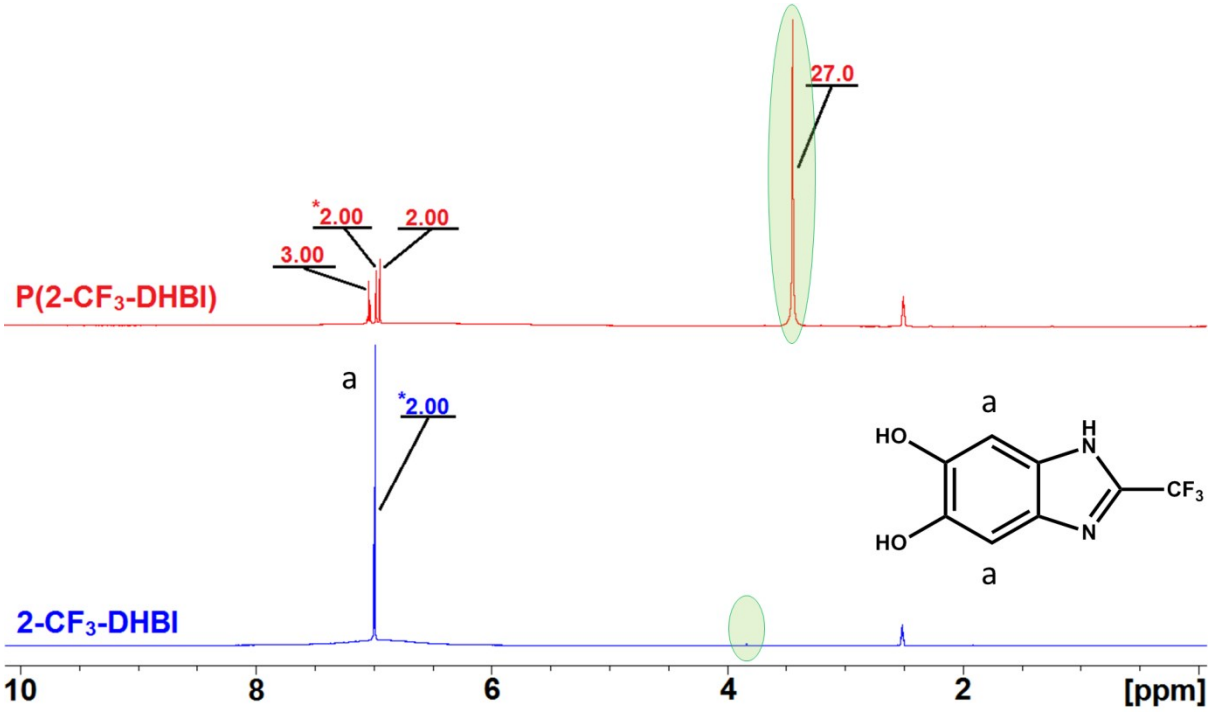

Fig. S10 Comparison of the ^{1}H NMR spectra of 2-CF_3-DHBI and P(2-CF_3-DHBI) – The ^{1}H of C-4 and C-7 was marked with (*), and the suspected peak originated from the residual methoxy group was highlighted by the green marker.

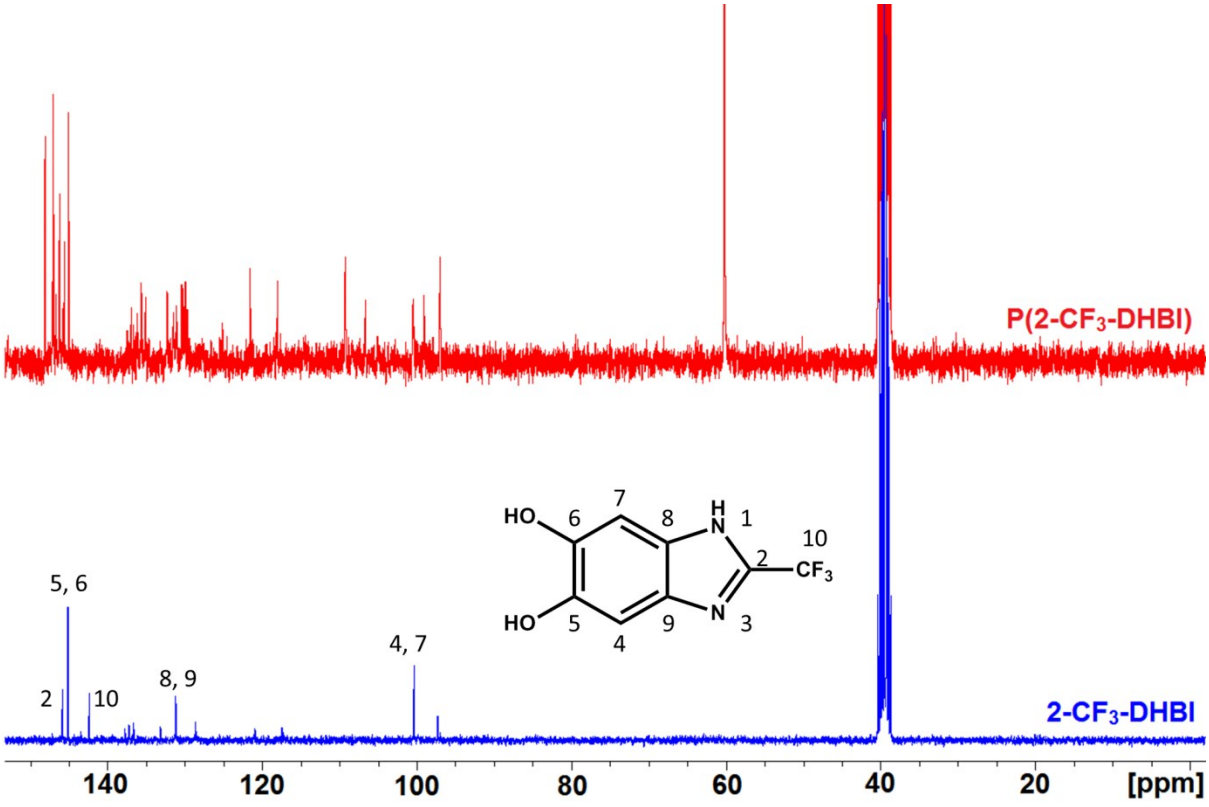

Fig. S11 Comparison of the ^{13}C NMR spectra of 2-CF_3-DHBI and P(2-CF_3-DHBI).

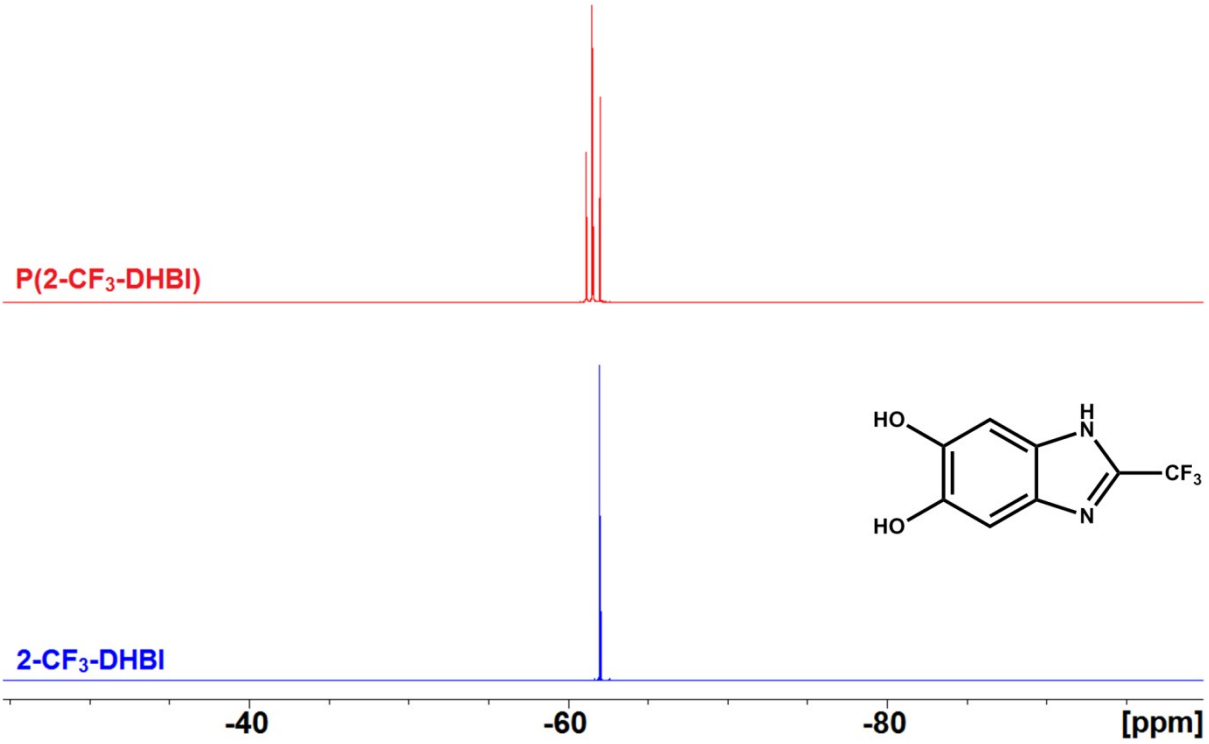

Fig. S12 Comparison of the ^{19}F NMR spectra of 2-CF_3-DHBI and P(2-CF_3-DHBI).

Table S2 Molecular weight and dispersity of the soluble fraction of the prepared DHBI-based polymers.

Sample	M_n, g mol^{-1}	M_w, g mol^{-1}	Dispersity, *Đ*
PDHBI	15,731	23,024	1.46
P(2-Me-DHBI)	15,181	36,844	2.43
P(2-CF_3-DHBI)	10,816	14,089	1.30

Table S3 Particle analysis of polymer coatings obtained from DLS and TGA.

	DLS Results		*TGA Results*
Sample	**Diameter (intensity), nm**	**Zeta Potential, mV**	**Average Degradable Content, %**
Silica	108	-36.3	N/A
PDA@SiO_2	211	-36.8	20%
P(DHBI-DA)@SiO_2	290	-33.5	29%
PDHBI@SiO_2	208	-22.7	33%

Supporting References

1 Y. Zhang, B. Thingholm, K. N. Goldie, R. Ogaki and B. Städler, *Langmuir*, 2012, **28**, 17585-17592.